www.czasopisma.pan.pl PAN POLSKA AKADEMIA NAUK www.journals.pan.pl

Arch. Min. Sci. **65** (2020), 4, 751-767

Electronic version (in color) of this paper is available: http://mining.archives.pl

DOI 10.24425/ams.2020.134145

MAGDALENA ZIĘBA[1*], PIOTR KALISZ[1], MARCIN GRYGIEREK[2]

THE IMPACT OF MINING DEFORMATIONS ON ROAD PAVEMENTS REINFORCED WITH GEOSYNTHETICS

In this article, the issue of mining impact on road pavements and subgrade is presented, taking into account the interaction between geosynthetic reinforcement and unbound aggregate layers. Underground mining extraction causes continuous and discontinuous deformations of the pavement subgrade. Structural deformations in the form of ruts are associated with the compaction of granular layers under cyclic loading induced by heavy vehicles. Horizontal tensile strains cause the loosening of the subgrade and base layers. The granular layers under cyclic loading are additionally compacted and the depth of ruts increases. Moreover, tensile strains can cause discontinuous deformations that affect the pavement in the form of cracks and crevices. Discontinuous deformations also affect the pavement in the fault zones during the impact of mining extraction. The use of geosynthetic reinforcement enables the mitigation of the adverse effects of horizontal tensile strains. Horizontal compressive strains can cause surface wrinkling and bumps. Subsidence causes significant changes in the longitudinal and transverse inclination of road surface. Both examples of the laboratory test results of the impact of subgrade horizontal strains on reinforced aggregate layers and the selected example of the impact of mining deformation on road subgrade are presented in this article. The examples show the beneficial impact of the use of geosynthetic reinforcement to stabilize unbound aggregate layers in mining areas.

Keywords: road subgrade, mining area, horizontal strain, unbound aggregate, geosynthetic reinforcement, laboratory test

1. Introduction

Road pavements, improved subgrades and embankments are constructed with unbound aggregate layers, which are mechanically stabilized. Pavement aggregate layers and subgrades are mainly responsible for the development of the structural deformations and fatigue cracks

[1] CENTRAL MINING INSTITUTE, 1 GWARKÓW SQ., 40-166 KATOWICE, POLAND
[2] SILESIAN UNIVERSITY OF TECHNOLOGY, GLIWICE, POLAND

* Corresponding author: mzieba@gig.eu

observed in wheel tracks on the pavement surface. Structural deformations are described as structural ruts and fatigue cracks as longitudinal cracks. These kinds of damage to pavement are associated with the compaction of granular layers under the influence of the cyclic loading induced by heavy vehicles. The property assessment of mechanically stabilized granular layers is based on estimating the value of the resilient modulus that a given aggregate can reach and the vertical deformation as a function of the number of loads. The modulus value depends on the grain size of the aggregate mix, its moisture content [1] and compaction, and the condition of the subgrade. In mining areas, subgrade strains are one of the most important factors determining the behavior of unbound aggregate layers [2] and pavement damage.

The use of geosynthetic reinforcement improves the properties of unbound aggregate layers and enables the mitigation of the adverse effects of cyclic loading and horizontal tensile strains. The geosynthetic reinforcement of pavements is also affected by horizontal displacements and strains of the subgrade. These deformations are partially transferred through the geosynthetic reinforcement due to tangential forces acting under this reinforcement. Properly dimensioned geosynthetic reinforcement can significantly reduce the impact of mining subgrade deformations on the mechanical properties of pavement structural layers. Geosynthetics are used to reinforce pavements, both in the case of continuous and discontinuous mining deformations. It should be emphasized that especially in the case of discontinuous deformations, geosynthetics only minimize the impact of deformations, e.g. by the mitigation of sudden changes in the shape of the deformed subgrade. Proposals for design methods for protecting the subgrade against discontinuous deformations, such as sinkholes, are presented in [3-4].

Both examples of the laboratory test results of the impact of subgrade horizontal strains on reinforced aggregate layers and the selected example of the impact of mining deformations on road subgrade are presented in this article.

2. The impact of underground mining on roads

Underground mining extraction causes continuous and discontinuous deformations of road subgrade and road pavement. Above the extracted mining area the subgrade is under the impact of horizontal compression strain (the compression zone) and outside this area it is under the impact of horizontal tensile strain (the tensile zone). Horizontal compression and tensile strain cause horizontal soil compaction and loosening, respectively. In the subsidence trough, the subgrade is subjected to uneven vertical and horizontal displacements. These displacements cause tilts, curvatures and horizontal strains in the pavement. In the case of shallow mining, i.e. with a depth up to approximately 100 m, discontinuous surface deformations may cause discontinuous pavement deformations, such as cracks, in the tensile zone, surface thresholds, sinkholes [5]. Continuous deformations occur on the surface during deep mining, i.e. with a depth of over 100 m (Fig. 1). Unfortunately, repeated extraction at depths greater than 100 m may also be accompanied by discontinuous deformations. These deformations occur when the edges of the extraction panels in the subsequent seams reach the common edge [5]. The impact of deep underground mining with many panels along a road and the distribution of deformation indices according to the *Knothe-Budryk* theory [6] are shown schematically in Fig. 1.

Above the operating edge being displaced, the subgrade is subjected to horizontal loosening, then horizontal compacting, and once again horizontal loosening. If the distance to this edge is sufficiently large, the value of subgrade strains should reach the value of zero. However, one

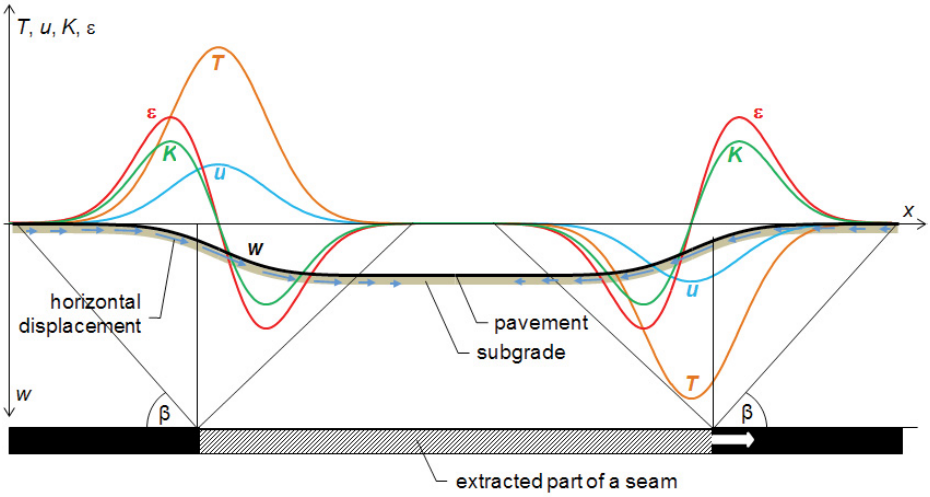

Fig. 1. The impact of underground mining extraction along a road and the distribution of deformation indices [6]: w – subsidence, T – tilt, u – horizontal displacement, K – curvature, ε – strain, where: β – angle of mining influence

study [7] showed that after the second horizontal loosening, the soil medium reaches an active limit state. In the zone around the constant edges of the extracted area, the soil is in a state of permanent strain [8].

The geosynthetic reinforcement of a pavement is affected by the horizontal strains of the subgrade. These strains are transferred to the pavement layers and geosynthetic reinforcement due to tangential forces induced below this reinforcement. The additional tensile stress and strain of the geosynthetics can adversely affect their bearing capacity and life cycle. The maximum values of additional tensile forces in the geosynthetic reinforcement depend on the value of the tangential forces between this reinforcement and the subgrade. The value of these forces depends on:

- the values of the subgrade displacements and strains as well as vertical load caused by the weight of the pavement and also the traffic load,
- the type of subgrade soil and its compaction,
- the type of geosynthetic reinforcement and its strength.

Geosynthetic reinforcement cannot counteract the compressive forces that occur in the zone of horizontal subgrade compaction. The subgrade strains during horizontal compaction are also transferred to the reinforced layers and may reduce the positive effects of geosynthetic use.

3. The mechanism of geosynthetic-aggregate layer interaction

Geosynthetics are widely used to improve the mechanical properties of the base layer of road pavements made of unbound aggregate. Depending on the polymer used and the structure of geosynthetics, the geosynthetics perform various functions [9], including reinforcement and stabilization.

Geosynthetics have viscoelastic-plastic properties because they are made of polymers. Elastic ε_e, viscous ε_v and plastic ε_p strains may occur simultaneously in polymers. Therefore, the stress value in polymers depends not only on the strain values but also on the history of the strain and load [10-12]. An example of the dependence of load on the strains in geogrids is shown in Figure 2.

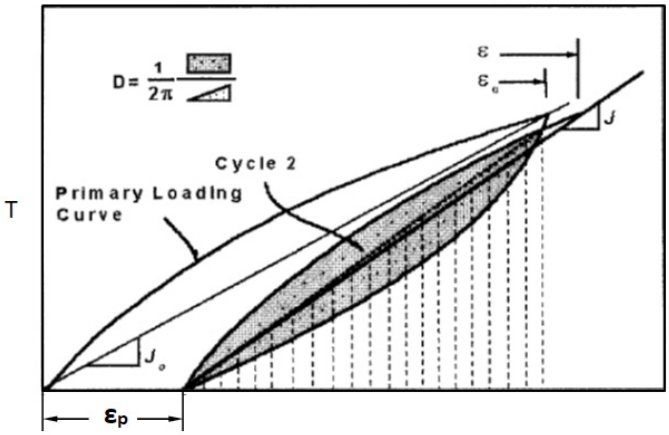

Fig. 2. Dependence of the longitudinal load on the strains in the first and second cycle of loading and unloading [10], T – load per unit width (kN/m)

Changeable loads, including cyclic loading generated by heavy traffic or rock mass tremors caused by mining, have a significant impact on geosynthetic features. The changeable loads of the geosynthetic reinforcement in mining areas are also caused by continuous deformations of the subgrade, but these occur over a much longer period of time and can be similar to those presented in Figure 2. Research on the geosynthetics properties under the influence of cyclic loading [10] shows that their strength does not significantly decrease. However, plastic deformations do occur. Exemplary cyclic load-strain dependences for polypropylene (PP) and polyester (PET) geogrid samples are presented in Figure 3.

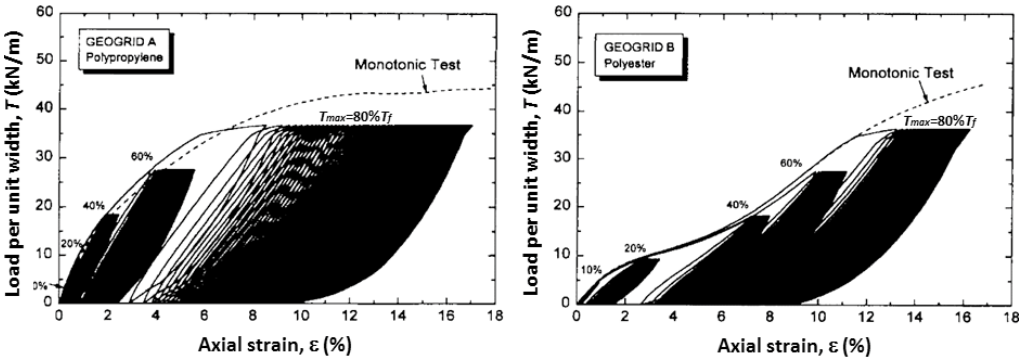

Fig. 3. Results of cyclic loading of PP and PET geogrid samples (with no aggregate) [10], T_f – tensile strength

Research on the geogrids under the influence of tensile forces with and without aggregate is presented in Fig. 4 [13].

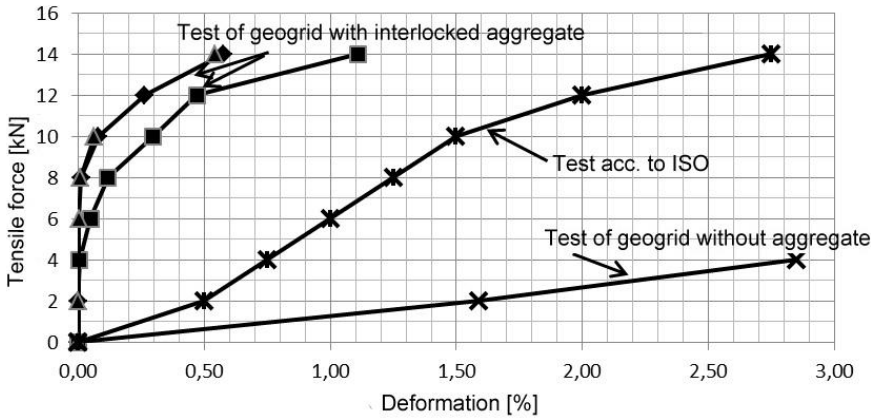

Fig. 4. Dependence of the stress on the geogrid deformation with and without aggregate [13]

Geosynthetics with a reinforcing function are designed to improve the load capacity of a weak subgrade. Requirements for these geosynthetics are characterized by the membrane effect. An important parameter characterizing the reinforcing function is the tensile strength of the geosynthetic, which is determined for a period of 120 years. The role of this function is to provide the geosynthetic with a continuous state of tensile stress so that the "tight" geosynthetic relieves the subgrade below it. Geogrids and geotextiles are included in this group of geosynthetics (Fig. 5).

Further mechanisms of the geosynthetic are associated with the restraint of aggregate grains. These mechanisms relate to the aggregate lateral restraint and improvement of the shear resistance of the aggregate layer, as demonstrated by the results of tests [13-16]. Unrestrained aggregate grains under load try to move, increasing the voids between the grains and thus weakening the stiffness of the layer. In order to reinforce the aggregate layer, it is necessary for the geosynthetic to significantly reduce grain displacement within the range of small strains. In these cases, the high stiffness of the geosynthetic in the range of the small strains is significant [13]. This stiffness is determined by the construction of intersecting ribs which form the geosynthetic structure, their thickness and their stiffness. The best properties in relation to the abovementioned mechanisms

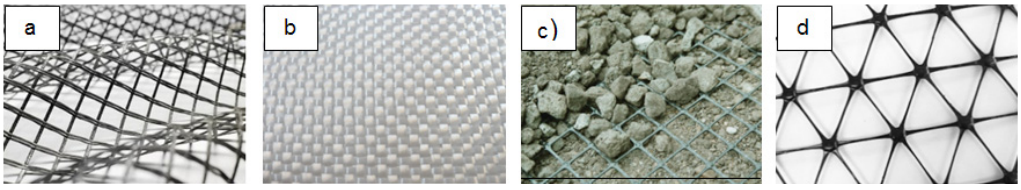

Fig. 5. Geosynthetics with a reinforcing and stabilizing function for unbound aggregate:
a) geogrid; b) geotextile; geogrid with rigid monolithic nodes – c) biaxial, d) triaxial [26]

are shown by monolithic geogrids, which include biaxial and triaxial geogrids (Fig. 5). Geogrids with the construction of stiff nodes and ribs, which enable the lateral restraint of aggregate grains, are attributed to the stabilizing function for unbound aggregate. The effectiveness of the lateral restraint of the aggregate grains in the geogrid meshes is a function of the distance from the meshing plane and it decreases as the distance from this plane increases. This mechanism is described in research [9,14-25].

Fig. 6 shows the working mechanisms of the geosynthetic that are associated with the reinforcing function and the improvement of the shear resistance of the aggregate layer.

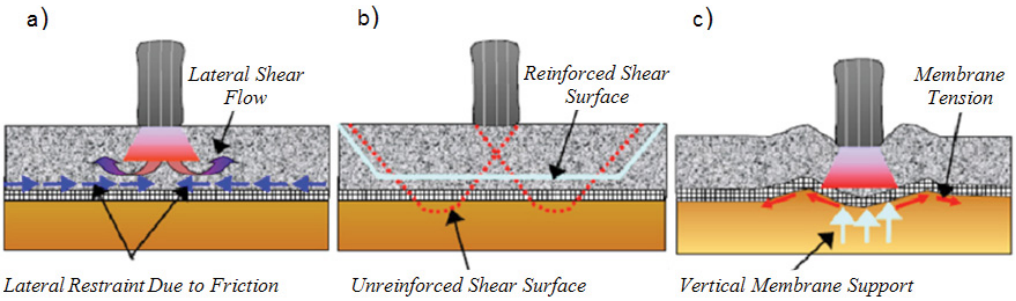

Fig. 6. Reinforcement mechanisms associated with the geosynthetics: (a) lateral restraint, (b) increased bearing capacity, and (c) membrane support [17]

4. Laboratory research of the impact of the subgrade strains on the geosynthetic reinforcement of unbound aggregate

The simulation of the impact of horizontal soil strains on the geosynthetic reinforcement took place in laboratory tests. These tests were performed in the laboratory test stand which the basic element is a rigid box of 1.2 m length and 1.0 m width. This box has two fixed walls and two movable walls (Fig. 7). The test stand box was being filled in with three layers of the burned shale aggregate to a total height of 0.5 m and a few centimeters above movable walls. The aggregate was laid with layers of about 20 cm thickness and compacted to obtain adequate compaction,

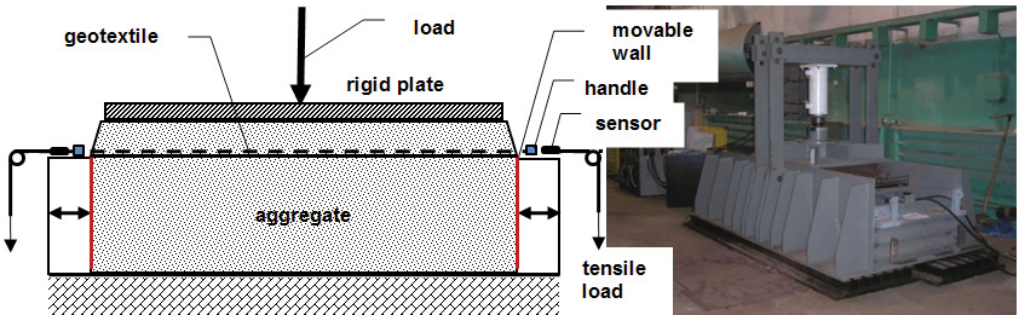

Fig. 7. Laboratory test stand

uniform for all tests. Geosynthetic material was laid on an evened aggregate surface and the pretension of 300 N was induced through handles mounted on the both sides of the geosynthetic sample. Measurements of the length changes of the geosynthetic sample were conducted using displacement sensors attached to the handles on the both sides of the sample. Then the compacted aggregate layer of 0.2 m thickness was laid on the geosynthetic. These tests were started with loading the reinforced aggregate layer to simulate the vertical unit load of 50 kPa with the use of a hydraulic actuator (Fig. 7).

The soil layer under the geosynthetic reinforcement was subjected to the impact of horizontal tensile strain, then horizontal compression strain, and once again horizontal tensile strain (the full cycle of soil straining simulated by the displacement of the movable walls). Changes in the average length of the geosynthetic samples were measured. The values of the horizontal subgrade strain were similar to in-situ values in mining areas. Exemplary test results for woven geogrids with different stiffness used to reinforce the burned shale aggregate are shown in Fig. 8. These two results show the dependencies of the geosynthetic reinforcement strains on the subgrade strains caused by mining impact. The stiffness (J_o according to Fig. 2) of the first geogrid of 95.6 kN/m is less than the stiffness of the second one of 288.1 kN/m. In the first case (sample 1, marked red in Fig. 8) the subgrade tensile strain increased to 14.5 mm/m this caused geogrid tensile strain of up to 6.05 mm/m and the subgrade compressive strain increased to −13.2 mm/m and this caused the compressive strain of the geogrid of up to −5.20 mm/m. After the full cycle of the subgrade straining, the geogrid is strained to 0.35 mm/m. In the second case (sample 2, marked blue in Fig. 8) the subgrade tensile strain increased to 15.1 mm/m caused geogrid tensile strain up to 3.25 mm/m and the subgrade compressive strain increased to −13.0 mm/m and this caused the compressive strain of the geogrid of up to −6.62 mm/m. After the full cycle of the subgrade straining, the geogrid is strained to −0.50 mm/m.

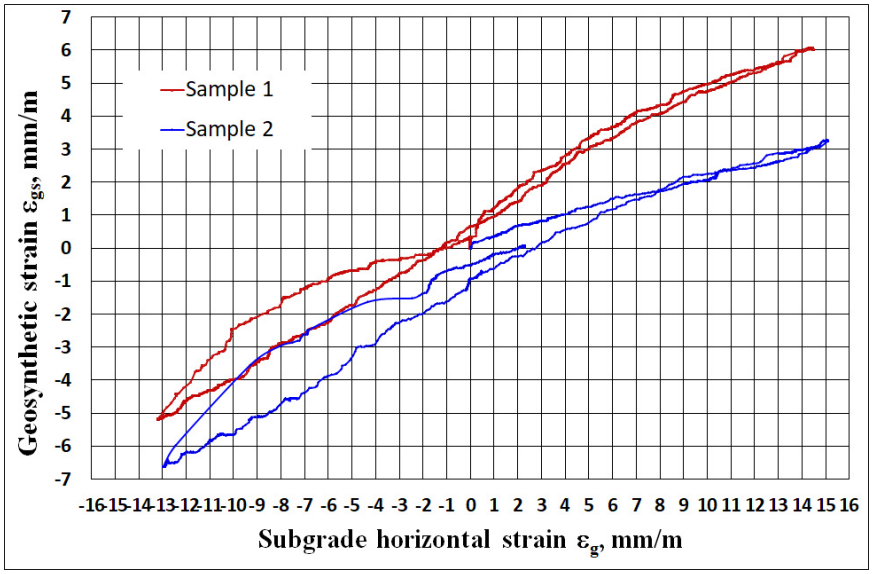

Fig. 8. Dependence of the PET geogrid strains on the subgrade soil strains

These two examples show the mitigation effect of the geosynthetic reinforcement use in the pavement construction in mining areas. The aggregate layer strains above the geogrids are less than the subgrade strains and even lower for higher stiffness of geogrid.

The similar issues related to the effectiveness assessment of the use of geosynthetics in continuous deformation areas are the subject of [27-28], and [29] concerns the discontinuous deformation areas.

5. Field research of the impact of mining subgrade deformations on the geosynthetic reinforcement of unbound aggregate

5.1. Characteristics of the road pavement

The assessment of the effectiveness of reinforcing the pavement with a geosynthetic was conducted on an area of road with a high traffic load which was also under the impact of discontinuous mining deformations. The road has a 1×2 cross section (one roadway with two lanes). In the cross section there is a hardened roadside with a construction which is similar to the lanes.

The pavement construction consists of several sections in which the system of layers differs in terms of thickness and the type of material layers adjusted to the predicted mining deformations. The system of layers in individual sections is shown in Fig. 9 and Table 1.

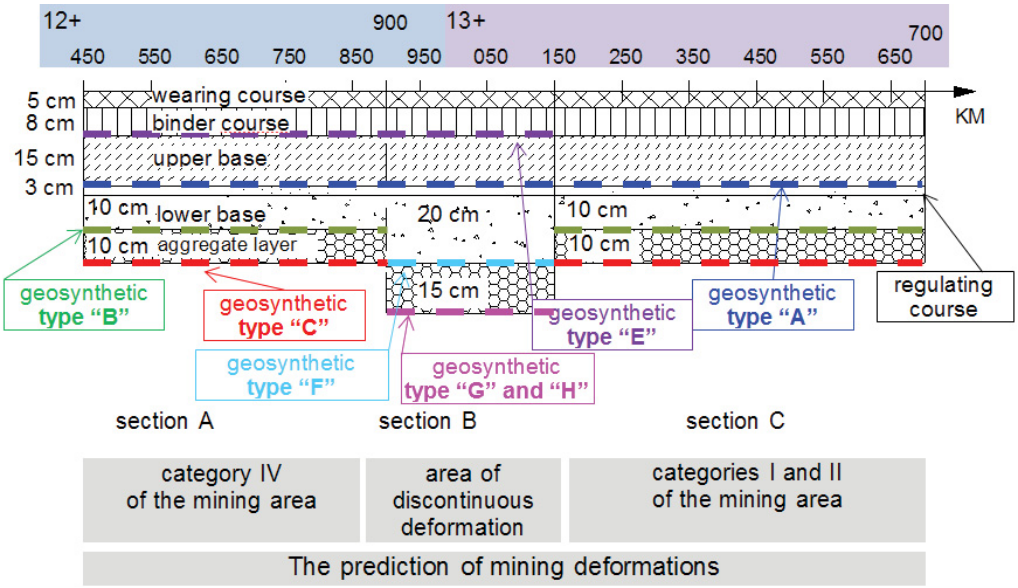

Fig. 9. Characteristics of pavement construction

TABLE 1

System and thickness of pavement layers for the selected road section

Number of the layer	Section A	Section B	Section C
	Thickness / kind of layer	Thickness / kind of layer	Thickness / kind of layer
1	5 cm / SMA 0/12.8	5 cm / SMA 0/12.8	5 cm / SMA 0/12.8
2	8 cm / BA 0/25	8 cm / BA 0/25	8 cm / BA 0/25
3	geosynthetic – type E	geosynthetic – type E	–
4	15 cm / BA 0/25	15 cm / BA 0/25	15 cm / BA 0/25
5	geosynthetic – type A	geosynthetic – type A	geosynthetic – type A
6	3 cm / BA 0/8	3 cm / BA 0/8	3 cm / BA 0/8
7	10 cm / KŁSM 4/31.5	20 cm / KŁSM 4/31.5	10 cm / KŁSM 4/31.5
8	geosynthetic – type B	geosynthetic – type F	geosynthetic – type B
9	10 cm / KNSM 8/31.5	15 cm / KNSM 8/31.5	10 cm / KNSM 8/31.5
10	geosynthetic – type C	geosynthetic – type G	geosynthetic – type C
11	–	geosynthetic – type H	–

Legend: SMA 0/12.8 – Stone Mastic Asphalt with a grain size of 0/12.8 mm, BA 0/25 – asphalt concrete with a grain size of 0/25 mm, KŁSM 4/31.5 – mechanically stabilized crushed aggregate with a grain size of 4/31.5 mm, KNSM 8/31.5 – mechanically stabilized natural aggregate with a grain size of 8/31.5. Geosynthetic: type A and E: geogrid+nonwoven geotextile, polymer: PET, ultimate tensile 50/50 kN/m, elongation at ultimate strength: 12/12%; type B: geogrid, PET, 65/65 kN/m, 10/10%; type C: nonwoven geotextile, PET, 25/25 kN/m, 15/15%; type F: geogrid, PET, 110/110 kN/m, 13/13%; type G: geogrid, PET, 110/110 kN/m, 13/13%; type H: nonwoven geotextile PP, 16/16 kN/m, 50/50%

5.2. Characteristics of mining conditions

The selected road section of the state road is located in a fault zone from km 12+800 to km 14+100 (marked blue in Fig. 10). The road section was subjected to mining impact from longwall

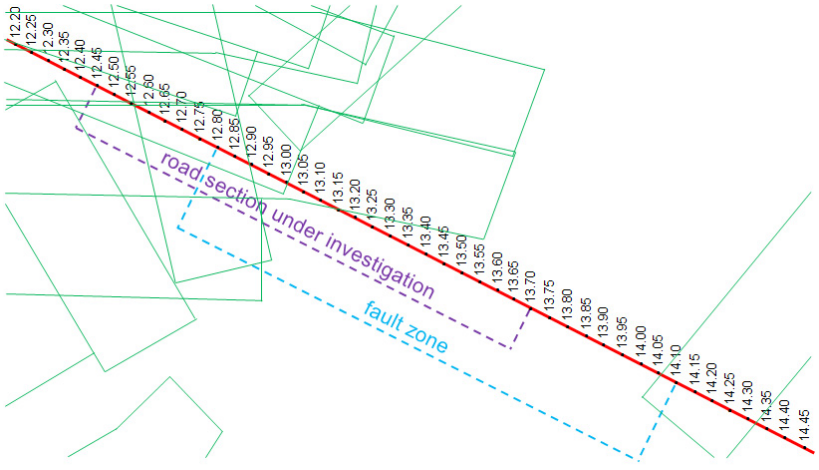

Fig. 10. Location of the selected road section against the background of the fault zone and the predicted mining

panel extraction (marked green in Fig. 10). The road section from km 12+450 to km 13+700 is under investigation (marked violet in Fig. 10).

5.3. Inventory of damage to the rebuilt road surface

Mining exploitation which was carried out after the completion of road reconstruction in 2006 caused discontinuous deformations on the pavement. These deformations caused corrugations in the pavement and also depressions in the form of local troughs (Fig. 11). The observed damage caused significant deterioration in the evenness of the pavement – both longitudinal and transverse. Cracks also appeared in the pavement (Fig. 11), mainly in the longitudinal direction. A characteristic delamination of the technological seam of the pavement, which occurs in the road axis, was also observed.

Fig. 11. Corrugations and local depressions of the road pavement (~km 12+750)

5.4. Assessment of the bearing capacity of the pavement

The bearing capacity of the pavement was assessed after damage occurred and was based on the measurement of pavement deflections with an FWD (Falling Weight Deflectometer). The measurement was conducted in the track of the right wheel, every 25 m, using a test load of 80 kN. The temperature of the mix asphalt layers during the tests was approximately +3°C. The calculated deflection values, standardized to a test force of 50 kN, are presented in Fig. 12. Identification of pavement layer modules was performed on the basis of data from deflection measurement. The adopted pavement models are shown in Table 2. The modules were identified using the ELMOD program (Figs. 13-15). The reliable module values were calculated as 0.85 quantile of all values in a given section (Table 2).

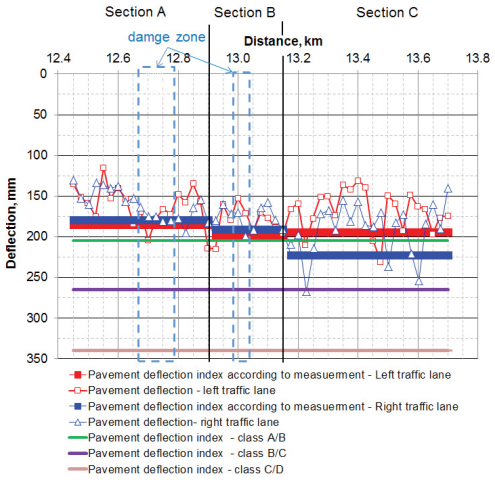

Fig. 12. Deflection of the pavement – case B

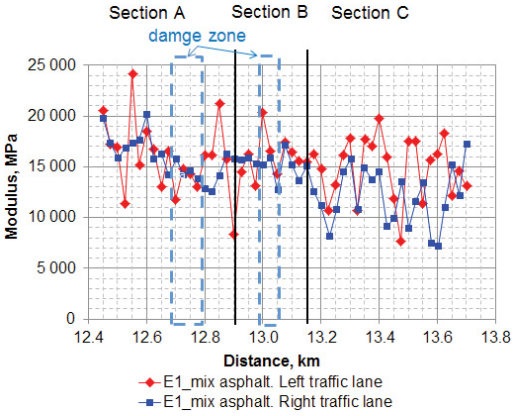

Fig. 13. Modules of the mix asphalt

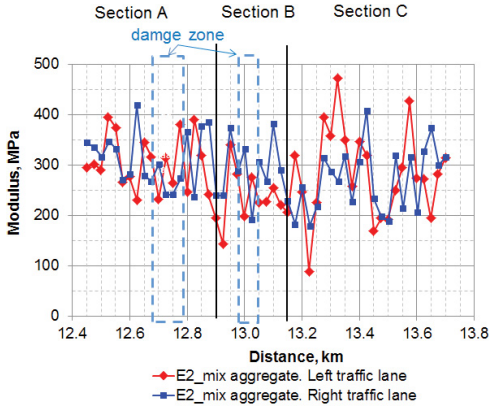

Fig. 14. Modules of the mix aggregate

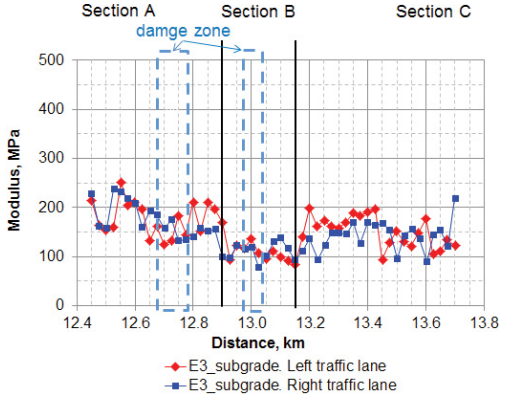

Fig. 15. Modules of the subgrade

TABLE 2

Computational models when identifying modules

Thickness / kind of layer	Section A		Section B		Section C	
	Thickness, cm	Reliable module values, MPa; L / P	Thickness, cm	Reliable module values, MPa;	Thickness, cm	Reliable module values, MPa; L / P
Mix asphalt	31	12 632 / 14 065	31	14 379 / 14 150	31	11 452 / 8 969
Mix aggregate	20	238 / 241	35	200 / 232	20	194 / 198
Subbase	∞	141 / 138	∞	93 / 95	∞	120 / 112

5.5. Calculation of pavement fatigue life

The calculations were conducted based on the criteria recommended in Poland for dimensioning a pavement, i.e. the AASHTO 2004 method for the assessment of the fatigue life of asphalt layers and the Asphalt Institute method for the assessment of the structural deformations of the ground [30-33]. The value of the fatigue life N_{asf} (the number of equivalent standard axles) of asphalt layers is calculated according to the formula

$$N_{asf} = 7.3557 \cdot \left(10^{-6}\right) \cdot C \cdot k_1^{'} \cdot \left(\varepsilon_t^{-3.9492}\right) \cdot E^{-1.281} \tag{1}$$

where:

$$C = 10^{M} \tag{2}$$

$$M = 4.84 \cdot \left(\frac{V_b}{V_a + V_b} - 0.69\right) \tag{3}$$

$$k_1^{'} = \frac{1}{0.000398 + \dfrac{0.003602}{1 + e^{(11.02 - 1.374 \cdot h_{ac})}}} \tag{4}$$

ε_t — tensile strain, μm/m,
E — stiffness modulus, MPa,
V_b — asphalt content by volume, %v/v,
V_a — air voids, % v/v,
h_{ac} — total thickness of bituminous layers, cm.

The criterion of the assessment of the subgrade strain ε_p, μm/m, according to the formula of the Asphalt Institute is

$$\varepsilon_p = 0.0105 \cdot N_{gr}^{-0.223} \tag{5}$$

where N_{gr} is the fatigue life (the number of equivalent standard axles).

The lowest value of N_{asf} and N_{gr} is considered as the fatigue life N_{min} of the pavement. The calculations of the values of strains ε_t and ε_p were conducted in the BISAR 3.0 program (elastic model) using the module values calculated based on the FWD measurements (Figs. 13-15). The values of modules $E2$ and $E3$ in the separated characteristic road sections are shown in Table 2. The stiffness modules of mix asphalt $E1$ (Table 2) were calculated with an equivalent temperature of +13°C (Table 3) [30]. Calculations were conducted with the thicknesses of the layers presented in Fig. 9. The pavement model was loaded with a standard axle with a load of 100 kN (50 kN per wheel) and a contact pressure of q = 850 kPa.

TABLE 3

Model parameters and the calculation results of the pavement fatigue life

Section	Traffic lane	Modulus, MPa			ε_t^*	ε_t^{**}	$\lvert\varepsilon_p\rvert$	$N_{asf\text{-}min}$	N_{gr}	N_{min}
		E1, MPa	E2, MPa	E3, MPa	µm/m	µm/m	µm/m	MSA***	MSA***	MSA***
A	Left	6 935	238	141	44.1	58.2	132	98.8	332	98.8
	Right	7 722	241	138	40.8	53.8	126	117.2	410	117.2
	Thickness, cm	31 cm	20 cm	∞						
B	Left	7 894	200	93	42.0	55.4	121	101.6	497	101.6
	Right	7 768	232	95	41.5	54.7	121	108.9	487	108.9
	Thickness, cm	31 cm	35 cm	∞						
C	Left	6 287	194	120	49.7	65.6	149	69.9	194	69.9
	Right	4 924	198	112	60.0	79.2	178	45.5	86	45.5
	Thickness, cm	31 cm	20 cm	∞						

* strain calculated at a depth of 28 cm, ** strain calculated at a depth of 31 cm, *** MSA – millions of standard axle loads100 kN

6. Assessment of the impact of the geosynthetic on the pavement properties in the area of discontinuous deformations

Geosynthetics (Table 1, Fig. 6) operating according to the membrane effect mechanism were used on the selected road section. The geosynthetic reinforcements were used both in aggregate layers and in mix asphalt. Based on the measurement of pavement deflections, it can be stated that the values of pavement deflections with the exception of the road section from km 13+150 to km 13+700 (right lane) are characterized by a reliable deflection index of lower than 205 µm (Fig. 12). This index, in terms of deflections, classifies the selected pavement in the highest class (class A) of load-bearing capacity for traffic KR6. It is worth noting that such a high load-bearing capacity was reached despite significant deformations and pavement damage (cracks). On the road section from km 13+150 to km 13+700 (right lane), the reliable deflection index is 223 µm and this results in this section being classified in load-bearing capacity class B. The class B categorization is sufficient, but it should be emphasized that there was no visible damage to this section during the measurement of deflections.

The identified module values in the overall assessment should be assessed as correct. The reliable values of the modules are slightly lower than those typical in layers with a good technical condition. However, in the case of the subbase, the values of the reliable modules in sections A and B are high, but in section B the value is slightly lower (93 MPa) than the required value of 120 MPa. In the case of layers of unbound aggregate, the reliable modules from 194 MPa to 238 MPa are lower than the values required at this level (400 MPa) [30]. It should be noted, however, that these layers are characterized by discontinuous graining (4/31.5), which is one of the main reasons for lower stiffness. In addition, it should also be highlighted that the adopted layer system is characterized by unusual, i.e. too thin, layer thicknesses (only 10 cm) which means

that it is unable to interact appropriately with the geosynthetic. Thicker aggregate layers (more than 10 cm) would certainly lead to more effective interaction with the geosynthetic.

Reliable modules of the mineral-asphalt mix at the measurement temperature are characterized by lower values (8,969 MPa-14,379 MPa) than typically occur at +3°C (>14,700 MPa). In the case of mix asphalt, lower values are justified due to the cracks observed in the pavement.

The fatigue life of the pavement calculated on the basis of field tests (Table 3) was compared to the fatigue life corresponding to the design assumptions (Table 4). This comparison (Fig. 16) shows that the fatigue life of the pavement in the area of the largest deformations (damage) was reduced, but by less than 20%. Greater reduction of the fatigue life (60%) occurs in section C where there were no discontinuous deformations. The reason for such significant differences in the reduction of the fatigue life is the lower modulus stiffness of the mix asphalt. Such low modulus stiffness may result, for example, from poor layer adhesion between the layers of the mix asphalt. Despite the lower fatigue life in section C, it should be noted that in all sections the pavement meets the requirements for traffic load KR6 (22 10^6 axle 100 kN < N_{min} < 52 106 axle 100 kN).

TABLE 4

Model parameters and calculations results of fatigue life

SECTION A and B							
Layer of pavement	**Thickness, cm**	**Modulus, MPa**	ε_t **µm/m**	$\lvert\varepsilon_p\rvert$ **µm/m**	N_{asf}, **MSA***	N_{gr}, **MSA***	N_{min}, **MSA***
Wearing course, SMA 0/12.8	5	8 360					117.1
Binder course, AC 0/25	8	8 240					
Base, AC 0/25	15	7 830	40.6		117.1		
Regulating course, AC 0/8	3	8 360	53.7		310.4		
Package of mix aggregate reinforced with geosynthetic	20	200					
Subgrade	∞	120		129		3700	
SECTION C							
Layer of pavement	**Thickness, cm**	**Modulus, MPa**	ε_t **µm/m**	$\lvert\varepsilon_p\rvert$ **µm/m**	N_{asf}, **MSA***	N_{gr}, **MSA***	N_{min}, **MSA***
Wearing course, SMA 0/12.8	5	8 360					126.6
Binder course, AC 0/25	8	8 240					
Base, AC 0/25	15	7 830	39.8		126.6		
Regulating course, AC 0/8	3	8 360	52.7		334.3		
Package of mix aggregate reinforced with geosynthetic	35	200					
Subgrade	∞	120		102		1040	

* MSA – millions of standard axle loads 100 kN

In the final assessment, the technical condition of the pavement should be assessed as very poor due to the unevenness of the pavement. In the case of layer stiffness, the technical condition of the pavement is assessed as sufficient, taking into account the scale of the pavement deformations. From the analyzed case, it can be concluded that the applied geosynthetic reinforcement package did not protect the pavement from damage to the mineral-asphalt mix. However, it contributed to stabilizing the stiffness of the mix of unbound aggregate layers at a sufficient

level. This effect is consistent with the observed results of laboratory tests which show that the loosening of the subgrade under the geosynthetic also causes elongation of the geosynthetic and, thus, the loosening of the layers built-in above it, but on a smaller scale than the situation in which a geosynthetic is not used. This conclusion is very useful, as it enables repairs of the pavement in the area with this type of deformations to take place. Properly reinforced subgrade, including the lower layers of the pavement, can be a sufficient load-bearing construction platform, thanks to which, after deformation, repair of mineral-asphalt layers can take place without interfering with the lower layers.

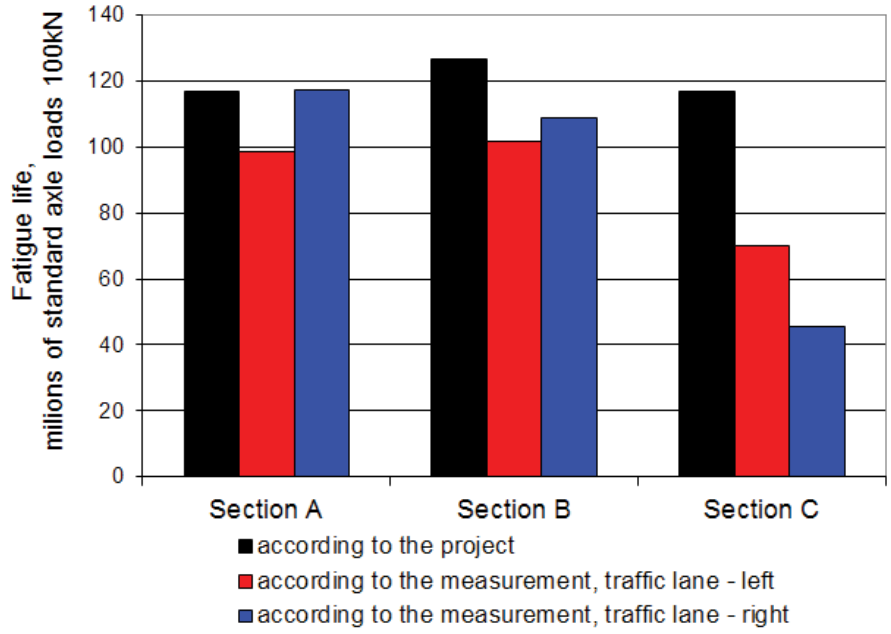

Fig. 16. Comparison of the designed pavement fatigue life which was calculated on the basis of deflection measurement

7. Conclusions

This article addresses the issue of mining impact on road pavements and subgrade, taking into account the interaction between geosynthetic reinforcement and unbound aggregate layers. The laboratory test results of the impact of subgrade horizontal strains on reinforced aggregate layers and the selected example of the impact of mining deformation on a road subgrade are presented.

According to the laboratory test results, geosynthetic reinforcements significantly reduce deformation of the overlying aggregate layer. This shows the beneficial effect of their use in pavement construction. However, it can be assumed that the maximum strains along the road are equal to the maximum horizontal strains of the subgrade.

Field tests in the area of discontinuous deformations, caused by mining, showed that the geosynthetics used retained high stiffness which was represented by the elasticity modulus of

the reinforced pavement layer. However, these geosynthetics did not protect the pavement surface from changes in its geometry, i.e. longitudinal and transverse evenness. In the case of discontinuous deformations, the geosynthetics are not always able to protect the pavement surface against tearing (cracks and crevices). In addition, in the case of such significant subgrade deformations, monitoring of geosynthetic effort should be considered using, for example, fiber optic sensors which are developing rapidly [34-35].

The results of research and analyzes enable to formulate the following recommendations for the design of pavement reinforcements in mining areas: (1) geomattress are a useful structural element reducing the adverse impact of mining deformations on the pavement, however it should be emphasized that they only minimize negative impacts, especially in the case of road geometry; (2) the reliable value of the geomattress's elastic modulus after significant deformations is about 200 MPa, but it is worth noting that the geomattress thickness should be about min. 30 cm; (3) when designing the geomattress, the nature of the geosynthetic work should be taken into account, which depends on its construction (type of nodes in the geogrid), quality of interaction with the aggregate filling it and the type of polymer used for its production (Figs. 5 and 6).

Acknowledgements

This study was performed in the framework of the research work in the Central Mining Institute [No. 11142019-132] and was financially supported by the Polish Ministry of Science and Higher Education.

References

[1] P. Rokitowski, M. Grygierek, *Initial research on mechanical response of unbound granular material under static load with various moisture content*. in IOP Conference Series: Materials Science and Engineering (2019).

[2] M. Grygierek, Drogi i Mosty **2**, 17-30 (2010).

[3] L. Briancon, P. Villard, Geotextiles and Geomembranes **26** (5) (2008), DOI: 10.1016/j.geotexmem.2007.12.00.

[4] P. Villard, A. Huckert, L. Briancon, Geotextiles and Geomembranes **44** (2016), DOI: 10.1016/j.geotexmem.2016.01.007

[5] M. Grygierek, M. Zięba, *Damage to road pavements in the area of linear discontinuous deformations on the surface caused by deep mining*. in: IOP Conf. Ser.: Earth Environ. Sci. **362** 012151 (2019), DOI: 10.1088/1755-1315/362/1/012151

[6] J. Kwiatek, *Obiekty budowlane na terenach górniczych* [in Polish]. Katowice: Główny Instytut Górnictwa (2007).

[7] W. Mika, PhD thesis, *Wpływ poziomych odkształceń podłoża górniczego na zmiany szerokości szczelin dylatacyjnych w budynkach dwusegmentowych* [in Polish], Katowice, Poland (1996).

[8] E. Popiołek, *Ochrona terenów górniczych* [in Polish], AGH, Kraków (2009).

[9] J.G. Zornberg, Procedia Engineering **189**, 298-306 (2017), DOI: 10.1016/j.proeng.2017.05.048

[10] H.I. Ling, Y. Mohri, T. Kawabata, Journal of Geotechnical and Geoenvironmental Engineering **124** (8), 782-787 (1998), DOI: 10.1061/(ASCE)1090-0241(1998)124:8(782)

[11] H.I. Ling, J.P. Wang, D. Leshchinsky, Geosynthetics International **15** (1), 14-21 (2008), DOI: 10.1680/gein.2008.15.1.14

[12] N. Moraci, G. Cardile, Geotextiles and Geomembranes. **27** (6), 475-487 (2009), DOI: 10.1016/j.geotexmem.2009.09.019

[13] M. Grygierek, J. Kawalec, Procedia Engineering **189**, 484-491 (2017), DOI: 10.1016/j.proeng.2017.05.078

[14] J.P. Giroud, J. Han, Geosynthetics **34** (1), 23-36 (2016).

[15] J. Han, J.P. Giroud, Geosynthetics **34** (3), 24-36 (2016).

[16] J. Han, J.P. Giroud, Geosynthetics **34** (2), 26-41 (2016).

[17] J.G. Zornberg, R. Gupta, *Geosynthetics in pavements: North American contributions*. in: 9th International Conference on Geosynthetics – Geosynthetics: Advanced Solutions for a Challenging World, ICG 2010, 379-400 (2010).

[18] Z. Rakowski, Procedia Engineering **189**, 166-173 (2017), DOI: 10.1016/j.proeng.2017.05.027

[19] Y. Qian, D. Mishra, E. Tutumluer, H.A. Kazmee, Geotextiles and Geomembranes **43** (5), 393-402 (2015), DOI: 10.1016/j.geotexmem.2015.04.012

[20] F. Horvat, S. Fischer, Z. Major, Acta Technica Jaurinensis **6**, 21-44 (2013).

[21] F. Horvat, J. Klompmaker, *Investigation of confinement effect by using the multi-level shear box test*. in: 10th International Conference on Geosynthetics, ICG 2014. Berlin, Germany (2014).

[22] T. Oliver, M. Wayne, J. Kwon, Procedia Engineering **143**, 896-910 (2016), DOI: 10.1016/j.proeng.2016.06.153

[23] M.H. Wayne, J. Kwon, D.J. White, *Assessment of pavement foundation stiffness using cyclic plate load test*. in: 10th International Conference on Geosynthetics, ICG 2014, 864-872, Berlin: Curran Associates, Inc. (2014).

[24] D.J. White, P.K.R. Vennapusa, Transportation Geotechnics **11**, 120-132 (2017), DOI: 10.1016/j.trgeo.2017.06.001

[25] J. Han, *Recent advances in geosynthetic stabilization of roads: Terminologies, products and mechanisms*. in: GA 2016 – 6th Asian Regional Conference on Geosynthetics: Geosynthetics for Infrastructure Development, Proceedings, KN17-KN33. New Delhi, India (2016).

[26] M. Grygierek, Acta Scientiarum Polonorum – Architectura **17** (4), 39-49 (2018), DOI: 10.22630/aspa.2018.17.4.39

[27] M. Al Heib, F. Emeriault, H.L. Nghiem, Journal of Rock Mechanics and Geotechnical Engineering **12** (1), 197-211 (2020), DOI: 10.1016/j.jrmge.2019.07.006

[28] M. Hassoun, P. Villard, M. Al Heib, F. Emeriault, International Journal of Geomechanics **18** (10) (2018), DOI: 10.1061/(ASCE)GM.1943-5622.0001265

[29] M.T. Pham, L. Briancon, D. Dias, A. Abdelouhab, Geotextiles and Geomembranes **46** (5) (2018), DOI: 10.1016/j.geotexmem.2018.04.015

[30] J. Judycki, P. Jaskuła, M. Pszczoła, D. Ryś, M. Jaczewski, J. Alenowicz, B. Dołżycki, M. Stienss, *New polish catalogue of typical flexible and semi-rigid pavements*. in MATEC Web of Conferences (2017), DOI: 10.1051/matecconf/201712204002

[31] W. Bańkowski, Appl. Sci. **8** (3), 469 (2018), DOI: 10.3390/app8030469

[32] J. Judycki, P. Jaskuła, M. Pszczoła, D. Ryś, M. Jaczewski, J. Alenowicz, B. Dołżycki, M. Stienss, *Analizy i projektowanie konstrukcji nawierzchni podatnych i półsztywnych* [in Polish]. Warszawa: Wydawnictwa Komunikacji i Łączności (2014).

[33] AASHTO, *Guide for mechanistic-empirical design of new and rehabilitated pavement structures*. Washington, DC: NCHRP (2004).

[34] Ł. Bednarski, R. Sieńko, T. Howiacki, M. Posłajko, Czasopismo Techniczne **3**, 73-85 (2017), DOI: 10.4467/2353737XCT.17.033.6344

[35] R. Sieńko, M. Zych, Ł. Bednarski, T. Howiacki, Structural Health Monitoring **18** (5-6), 1510-1526 (2019), DOI: 10.1177/1475921718804466